THE PROTEIN SOCIETY

The PNT domain from *Drosophila* Pointed-P2 contains a dynamic N-terminal helix preceded by a disordered phosphoacceptor sequence

Desmond K. W. Lau,[1,2] Mark Okon,[1,2] and Lawrence P. McIntosh[1,2,3]*

[1]Department of Biochemistry and Molecular Biology, University of British Columbia, Vancouver, British Columbia V6T 1Z3, Canada

[2]Department of Chemistry, University of British Columbia, Vancouver, British Columbia V6T 1Z1, Canada

[3]Michael Smith Laboratories, University of British Columbia, Vancouver, British Columbia V6T 1Z4, Canada

Received 12 July 2012; Revised 22 August 2012; Accepted 27 August 2012
DOI: 10.1002/pro.2151
Published online 30 August 2012 proteinscience.org

Abstract: Pointed-P2, the *Drosophila* ortholog of human ETS1 and ETS2, is a transcription factor involved in Ras/MAP kinase-regulated gene expression. In addition to a DNA-binding ETS domain, Pointed-P2 contains a PNT (or SAM) domain that serves as a docking module to enhance phosphorylation of an adjacent phosphoacceptor threonine by the ERK2 MAP kinase Rolled. Using NMR chemical shift, ^{15}N relaxation, and amide hydrogen exchange measurements, we demonstrate that the Pointed-P2 PNT domain contains a dynamic N-terminal helix H0 appended to a core conserved five-helix bundle diagnostic of the SAM domain fold. Neither the secondary structure nor dynamics of the PNT domain is perturbed significantly upon *in vitro* ERK2 phosphorylation of three threonine residues in a disordered sequence immediately preceding this domain. These data thus confirm that the *Drosophila* Pointed-P2 PNT domain and phosphoacceptors are highly similar to those of the well-characterized human ETS1 transcription factor. NMR-monitored titrations also revealed that the phosphoacceptors and helix H0, as well as region of the core helical bundle identified previously by mutational analyses as a kinase docking site, are selectively perturbed upon ERK2 binding by Pointed-P2. Based on a homology model derived from the ETS1 PNT domain, helix H0 is predicted to partially occlude the docking interface. Therefore, this dynamic helix must be displaced to allow both docking of the kinase, as well as binding of Mae, a *Drosophila* protein that negatively regulates Pointed-P2 by competing with the kinase for its docking site.

Keywords: transcription; Ras-dependent signal transduction; PNT domain; SAM domain; MAP kinase docking; phosphorylation; protein dynamics; hydrogen exchange; NMR spectroscopy

Introduction

Gene expression and signal transduction require tightly controlled macromolecular interactions and post-translational modifications involving both modular domains and intrinsically disordered regions of regulatory proteins. This paradigm is well exemplified by the ETS transcription factors. In addition to a conserved

Additional Supporting Information may be found in the online version of this article.

Grant sponsor: The Canadian Cancer Society Research Institute; Grant numbers: CCSRI 017308, 2011-700772; NMR instrumentation grant sponsors; The Canadian Institutes for Health Research (CIHR), The Canadian Foundation for Innovation (CFI), The British Columbia Knowledge Development Fund (BCKDF), The UBC Blusson Fund, The Michael Smith Foundation for Health Research (MSFHR).

*Correspondence to: Lawrence P. McIntosh, Department of Biochemistry and Molecular Biology, Life Sciences Centre, 2350 Health Sciences Mall, University of British Columbia, Vancouver, B.C., Canada, V6T 1Z3. E-mail: mcintosh@chem.ubc.ca

DNA-binding ETS domain, ~1/3 of all ETS factors also contain a PNT domain,[1] which is an ETS-specific member of the widespread family of SAM domains. Although sharing a common core architecture of four α-helices and a fifth small α- or 3_{10}-helix, SAM domains exhibit remarkably diverse association states and function in a wide variety of protein–protein and protein–RNA interactions.[2] Defining the molecular basis for this diversity remains an important challenge. In the case of the ETS factors, one source of specificity is provided by additional helices appended to the core SAM domain. The PNT domains of Yan, ETV6 (or Tel), ERG, ELF3, and FLI1 contain only the minimal helical bundle, whereas those of GABPA and SPDEF have one additional N-terminal helix[3] and those of ETS1 and ETS2 have two.[4] Furthermore, owing to differing surface features,[5] the PNT domains of Yan and ETV6 self-associate,[6,7] whereas the remainder are monomeric in isolation. Also, in disordered regions immediately preceding the PNT domains of closely related mammalian ETS1/ETS2 and *Drosophila melanogaster* Pointed-P2 are phosphoacceptors for the orthologous Ras-activated MAP kinases ERK2 and Rolled, respectively.[4,8,9]

The role of the ETS1 PNT domain in Ras/MAP kinase signaling has been investigated extensively using combination of cell-based and biophysical measurements. The monomeric PNT domain is a docking module for ERK2, enhancing the efficiency of phosphorylating Thr38 and Ser41 in a disordered region preceding this structured domain.[10,11] The docking interfaces on the PNT domain and the kinase have been mapped coarsely through mutagenesis, NMR spectroscopic, chemical footprinting, and competition studies.[10,12–15] To both accommodate the proposed docking mechanism and position the phosphoacceptors in the catalytic site of the kinase, a significant conformational change in the ETS1 PNT domain, such as the unfolding of the appended N-terminal helix H0 (residues Lys42-Thr52), appears to be required.[16] Indeed, NMR relaxation and amide hydrogen exchange (HX) measurement have shown that this helix is only marginally stable and structurally flexible.[4] Furthermore, upon phosphorylation, this helix H0 remains folded, but adopts a broad distribution of conformations displaced from the core helical bundle (H2–H5). This in turn contributes to enhanced electrostatically driven interactions with the TAZ1 domain of the general transcriptional coactivator acetyltransferase CBP, and ultimately, increased expression of Ras-responsive ETS1 target genes.[4,17]

Pointed-P2, the *Drosophila* ortholog of ETS1, plays a similar role in the well-characterized EGF and Sevenless receptor tyrosine kinase/Ras-mediated signal transduction pathway to control fly eye development.[18–21] Monomeric Pointed-P2 is a transcriptional activator and antagonist to Yan, an ETS family transcriptional repressor that polymerizes via head-to-tail self-association of its PNT/SAM domain.[7] Both control the expression of a common set of target genes, including a crucial regulator called Mae.[22] Upon stimulation of the receptor tyrosine kinase signaling cascade, the MAP kinase Rolled is activated and enters the nucleus to phosphorylate Yan, thereby leading to its CRM1-mediated export and subsequent cytoplasmic degradation.[23,24] This is facilitated by the SAM domain of Mae,[25] which acts as a tight-binding heterotypic partner of the Yan PNT/SAM domain to favor its depolymerization and to expose a critical phosphoacceptor site.[7] In parallel, Rolled phosphorylation of Pointed-P2 leads to transcriptional activation of the genes previously repressed by Yan. The PNT domain of Pointed-P2 is docking module for the kinase to enhance phosphorylation of the adjacent phosphoacceptor Thr151.[26] However, as part of a negative feedback mechanism, Mae also heterodimerizes with the PNT domain of Pointed-P2 to block kinase docking and hence down regulating phosphorylation-enhanced gene expression.[26] Parenthetically, recent studies have shown that mammalian TEL2 is functionally similar to Mae and can abrogate transcriptional output from ETS1/ETS2, albeit by a currently undefined mechanism.[27]

In this brief communication, we have used NMR spectroscopy to investigate further the similarities between the PNT domains and the phosphoacceptor regions of ETS1 and Pointed-P2 [Fig. 1(A)]. Based on main chain chemical shifts, the PNT domain of Pointed-P2 also contains additional helices H0/H1 appended to the core SAM helical bundle. NMR relaxation and amide HX studies confirm that these appended helices are dynamic and only marginally stable. Furthermore, rat ERK2 phosphorylates *in vitro* a Pointed-P2 fragment at three acceptor sites (Thr145, Thr151, and Thr154) in the disordered region immediately N-terminal to the PNT domain, and these post-translational modifications have, at best, only minor effects on the secondary structure and dynamics of the PNT domain. NMR-monitored titrations of Pointed-P2 with ERK2 also reveal that both the phosphoacceptor region and the PNT domain interact with the kinase. Based on these similarities, we hypothesize that the ETS1 and Pointed-P2 PNT domains share similar mechanisms of MAP kinase docking and recruitment of transcriptional coactivators.

Results

Pointed-P2 PNT domain contains a dynamic helix H0

The well-dispersed ^{15}N-HSQC spectrum of PntP2$^{142–252}$ confirms that the monomeric PNT domain-

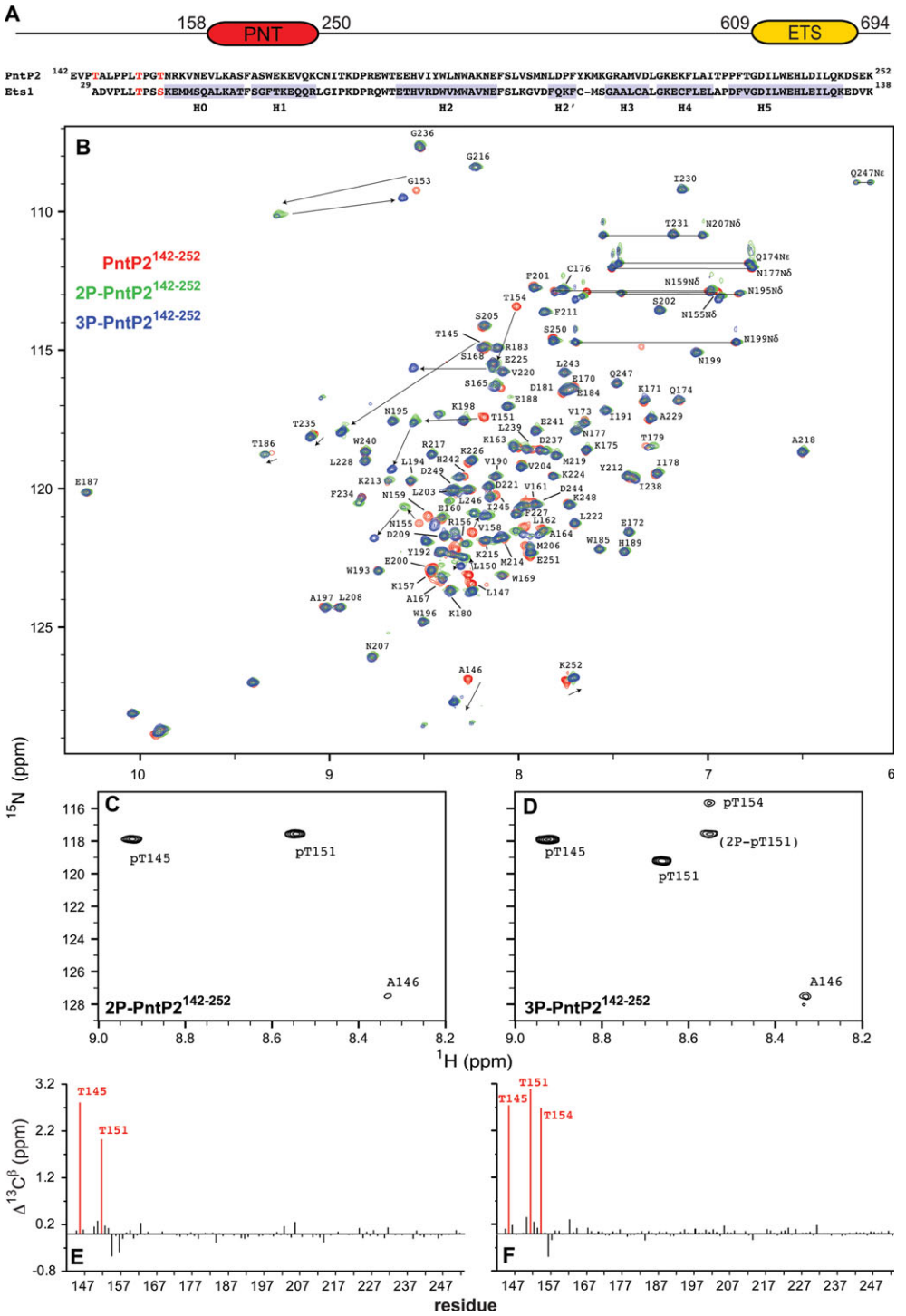

Figure 1. NMR spectroscopic characterization of PntP2$^{142–252}$. (A) Cartoon of the 718-residue Pointed-P2 transcription factor showing the structured PNT domain and DNA-binding ETS domain, along with aligned sequences of PntP2$^{142–252}$ and Ets1$^{29–138}$. The identified ERK2 phosphoacceptors are in red, and the observed consensus α-helices (or 3_{10}-helix for H2′) in the NMR-derived structural ensembles of Ets1$^{29–138}$ (2jv3.pdb) and 2P-Ets1$^{29–138}$ (2kmd.pdb) are shaded in light blue.[4] (B) Superimposed ^{15}N-HSQC spectra of PntP2$^{142–252}$ (red), 2P-PntP2$^{142–252}$ (green), and 3P-PntP2$^{142–252}$ (blue). The arrows indicate the progressive spectral perturbations upon increased phosphorylation. Amide signals from phosphothreonines are observed selectively in the ^{1}H–^{15}N faces of ^{31}P-edited HNCA spectra of (C) 2P-PntP2$^{142–252}$ and (D) 3P-PntP2$^{142–252}$. Although the latter experiment also detects the residue immediately following a phosphothreonine,[32] only Ala146 is observed as Pro152 lacks an amide $^{1}H^{N}$ and Asn155 has a relatively weak ^{15}N-HSQC signal. Owing to incomplete separation by anion exchange chromatography, resolved signals from contaminating 2P-PntP2$^{142–252}$ were observed in the spectra of 3P-PntP2$^{142–252}$ shown in (B and D). The phosphothreonines in (E) 2P-PntP2$^{142–252}$ and (F) 3P-PntP2$^{142–252}$ were also identified based on a large diagnostic downfield $^{13}C^{\beta}$ shift[33] relative to the corresponding unmodified amino acid in PntP2$^{142–252}$. [Color figure can be viewed in the online issue, which is available at wileyonlinelibrary.com.]

containing fragment of Pointed-P2 adopts an independently folded structure [Fig. 1(B)]. With the exception of Glu142, Val143, Phe166 and the N-terminal Gly-Ser-His-Met tag, almost complete $^{1}H^{N}$, ^{15}N, $^{13}C^{\alpha}$, $^{13}C^{\beta}$, and $^{13}C'$ resonance assignments were obtained for this construct. These chemical shifts were used to identify the secondary structural elements of PntP2$^{142–252}$ with the MICS (Motif Identification by Chemical Shift) algorithm.[28] Based on this analysis, PntP2$^{142–252}$ contains six helical regions that closely match those identified in Ets1$^{29–138}$ [Figs. 2(A,B)], as well as Ets2$^{69–172}$ (data not shown[4]). This strongly suggests that the PNT domains of Pointed-P2, ETS1, and ETS2 also share a common tertiary structure of a SAM core (helices H2–H5) with appended N-terminal helices H0/H1. In the NMR-derived structural ensemble of Ets1$^{29–138}$, these two appended helices are essentially continuous, yet bend at Phe53 to allow extended packing against the core helices H2 and H5. The corresponding residue in PntP2$^{142–252}$ is Phe166.

The dynamic properties of PntP2$^{142–252}$ were examined using ^{15}N relaxation and amide HX measurements. As shown in Figure 3(A), the heteronuclear ^{15}N-NOE values of residues in helix H0 progressively decrease toward its N-terminus. A model-free analysis of the ^{15}N T_1, T_2, and NOE values of PntP2$^{142–252}$ shows a similar trend with lower S^2 order parameters for amides near the start of this helix, as well as at the C-terminus of helix H5 (Supporting Information Fig. 1S). These data are indicative of enhanced backbone mobility on a nsec–psec timescale relative to the well-ordered SAM core. However, it is difficult to estimate the nature of the conformations sampled by these fast motions from ^{15}N relaxation measurements alone.[30] More importantly, rapid amide HX was detected for residues throughout helices H0/H1 [Fig. 4(A)]. The measured HX rate constants for these residues are comparable to those predicted for an unstructured polypeptide under similar conditions.[31] The only other regions of the PntP2$^{142–252}$ showing such behavior are the disordered termini and exposed loops, as the remaining amides in the structured PNT domain exchange too slowly to be detected by the CLEANEX magnetization transfer approach. This clearly demonstrates that helices H0/H1 are only marginally stable and must undergo substantial local unfolding to allow facile exchange with water. Very similar ^{15}N relaxation and HX behavior was observed for helix H0 in Ets1$^{29–138}$, indicating that the PNT domains of these two ETS family members also exhibit common dynamic properties.[4]

Pointed-P2 PNT domain phosphoacceptors are disordered

The effect of phosphorylation on the properties of Pointed-P2 was examined using active ERK2 to

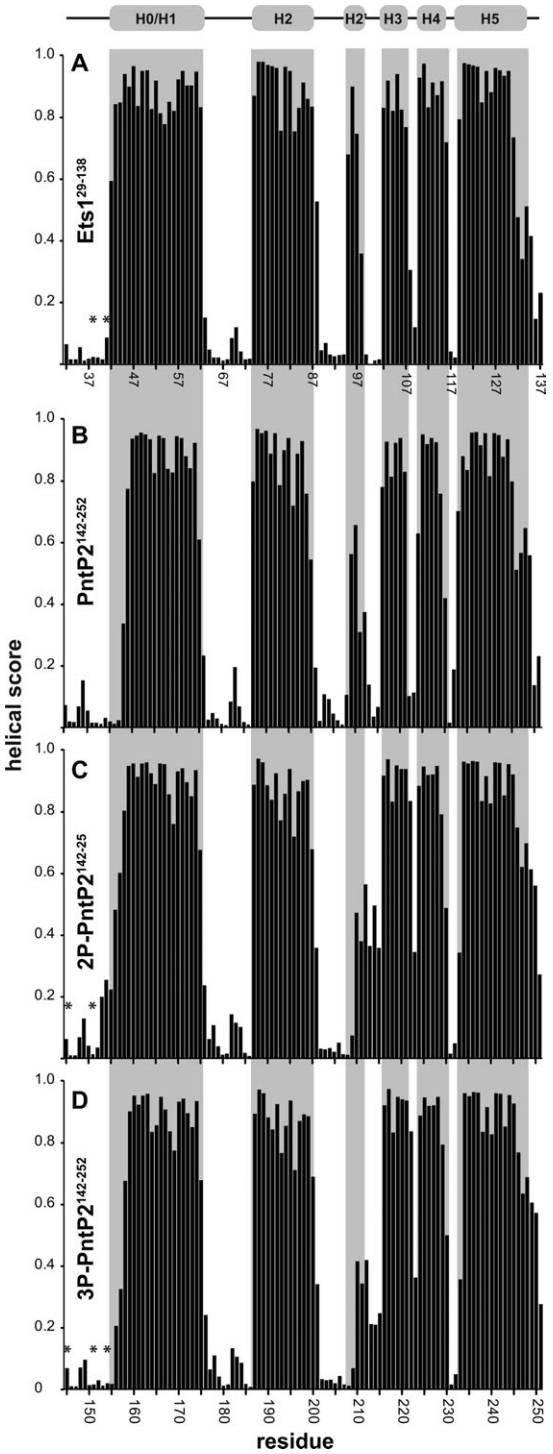

Figure 2. The PNT domains of PntP2 and Ets1 share similar helical secondary structures. Shown are the predicted helical scores for (A) 2P-Ets1$^{29–138}$ (data from Ref. 4), (B) PntP2$^{142–252}$, (C) 2P-PntP2$^{142–252}$, and (D) 3P-PntP2$^{142–252}$, based on an analysis of $^{1}H^{N}$, ^{15}N, $^{13}C^{\alpha}$, $^{13}C^{\beta}$, and/or $^{13}C'$ chemical shifts using the program MICS.[28] Consideration of phosphorylation-dependent chemical shift changes[33] does not significantly alter the scores for the phosphoacceptor serines/threonines (asterisks). The top cartoon and the gray rectangles indicate the observed consensus α-helices (or 3_{10}-helix for H2′) in the NMR-derived structural ensembles of Ets1$^{29–138}$ (2JV3.pdb) and 2P-Ets1$^{29–138}$ (2KMD.pdb).[4]

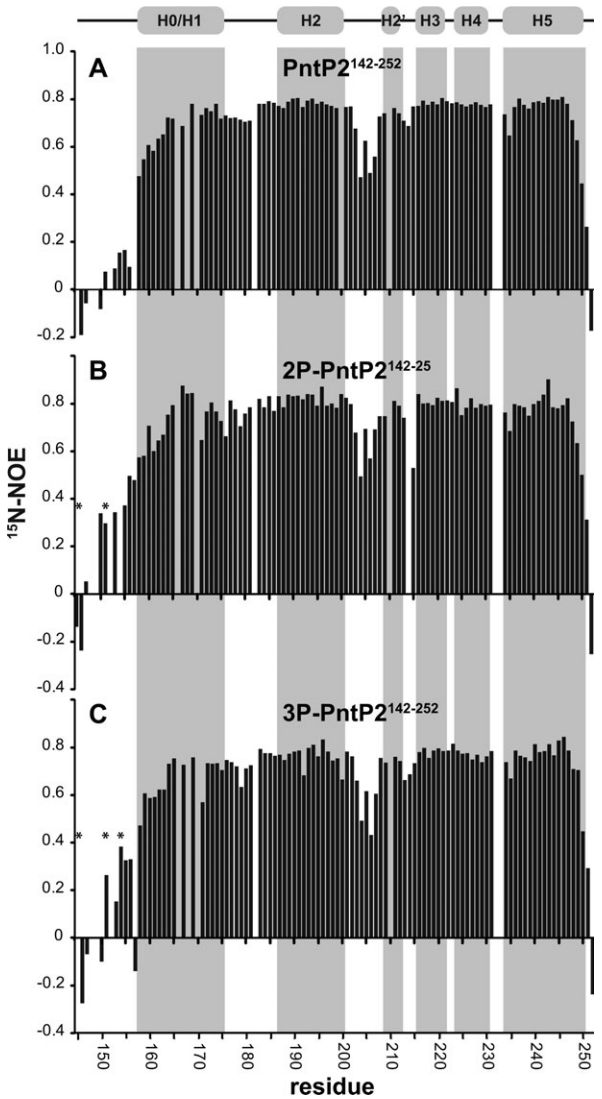

Figure 3. PntP2$^{142–252}$ phosphoacceptors and helix H0 are flexible. Steady-state heteronuclear ^{15}N-NOE values for (A) PntP2$^{142–252}$, (B) 2P-PntP2$^{142–252}$, and (C) 3P-PntP2$^{142–252}$. Well-ordered residues have NOE values of ~0.8, whereas decreasing values indicate increasing mobility of the ^{15}N–^{1}H^{N} bond vector on the nsec–psec timescale.[29] The top cartoon and the gray rectangles indicate the helices, based on the consensus MICS scores, for the three PntP2$^{142–252}$ species [H0/H1, 158–175; H2, 187–200; H2′, 209–212; H3, 216–221; H4, 224–230; H5, 234–250; Figs. 2(B–D)], and the phosphothreonines are identified with asterisks. Missing data correspond to prolines or residues with overlapping signals. The error is ~5%.

post-translationally modify PntP2$^{142–252}$ *in vitro*. Treatment with the kinase yielded products with two or three phosphorylated residues. The sites of modification were identified unambiguously via complementary NMR spectroscopic methods. The first method exploits a weak two-bond ^{31}P–^{13}C$^{\alpha}$ scalar coupling to selectively detect the amide ^{1}H^{N}–^{15}N signals from a phosphorylated serine/threonine (i) and its (i + 1) neighbor via a ^{31}P-edited HNCA spectrum [Figs. 1(B,C)].[32] The second relies on the observation that the ^{13}C$^{\beta}$ signal of a random coil serine/threonine shifts downfield by ~2–4 ppm upon phosphorylation [Figs. 1(D,E)].[33] Based on these measurements,

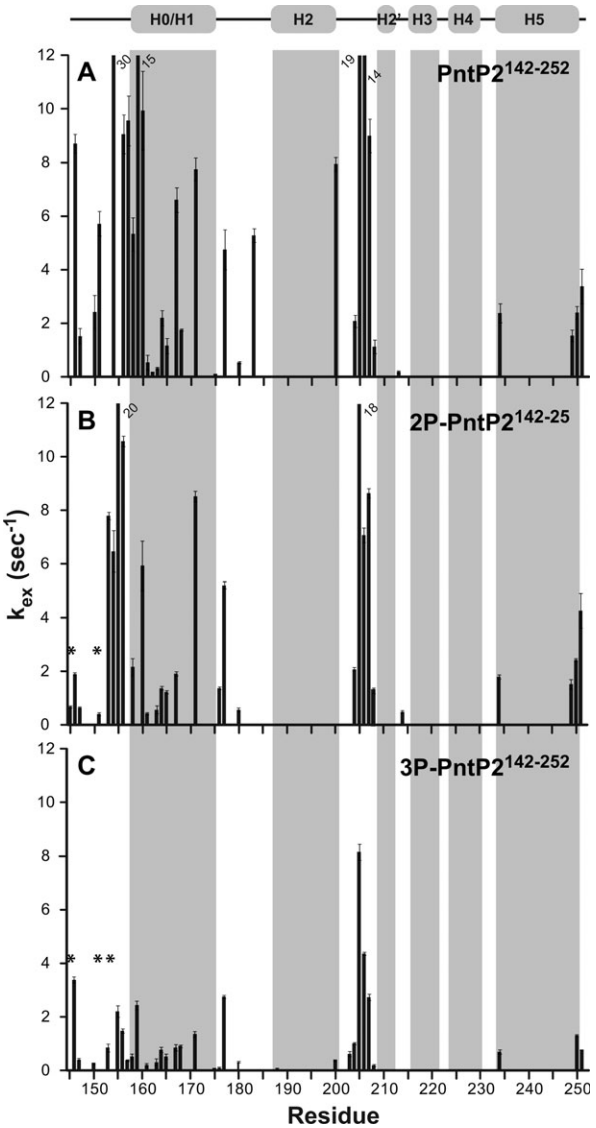

Figure 4. Helices H0/H1 are marginally stable with little protection from HX. Amide HX rate constants were determined from CLEANEX experiments recorded at 25°C for (A) PntP2$^{142–252}$ (pH 6.7 and pH 7.5), (B) 2P-PntP2$^{142–252}$ (pH 6.7), and (C) 3P-PntP2$^{142–252}$ (pH 7.1 and 7.5), and normalized to pH 6.7, assuming a first-order dependence on [OH^{-}]. For better comparison, the bars for several data points were truncated and the rate constants indicated by the numbers. Phosphothreonines are identified with asterisks. Missing data points correspond to prolines, amides with overlapping ^{15}N-HSQC signals, and amides with HX rates too slow to be measured by the CLEANEX approach under the sample pH conditions examined (i.e., $k_{ex} < 0.5\ s^{-1}$). Most amides fall in the latter category owing to their presence in stable, hydrogen-bonded structural elements of the protein. However, in the case of 3P-PntP2$^{142–252}$, the three phosphothreonines likely exchange rapidly but were not included in (C) owing to ambiguous spectral assignments at elevated sample pH values.

2P-PntP2$^{142–252}$ is clearly phosphorylated at both Thr145 and Thr151, whereas 3P-PntP2$^{142–252}$ contains an additional modification at Thr154. Of these phosphoacceptors, only Thr151 is within a MAP kinase consensus sequence (Pro-x-Ser/Thr-Pro).[34,35]

The phosphoacceptor threonines of PntP2$^{142–252}$ are within the disordered region N-terminal to the helical PNT domain. Similar to Ets1$^{29–138}$,[4] the conformational flexibility of these residues is evident from both random coil chemical shifts [Fig. 2(B)], low heteronuclear ^{15}N-NOE values [Fig. 3(B)], and rapid HX [Fig. 4(A)]. Furthermore, phosphorylation does not induce any predominant secondary structure for this region of the Pointed-P2 fragment [Figs. 2(C,D)] and only slightly dampens fast nsec–psec timescale motions of pThr151 and pThr154 detectable via ^{15}N-NOE measurements [Figs. 3(B,C)].

Phosphorylation of PntP2$^{142–252}$ has also no pronounced effect on the structure or dynamics of the PNT domain. A comparison of ^{15}N-HSQC spectra reveals that amide chemical shift perturbations owing to phosphorylation are localized to residues near the phosphoacceptors [Figs. 1(A,D,E) and Supporting Information Fig. 2S]. Thus, the structure of the PNT domain is not altered upon modification of the threonines. A small increase in the MICS–helical scores of residues 155–157 is noted in 2P-PntP2$^{142–252}$, presumably owing to phosphorylation of Thr151, yet these values decrease in 3P-PntP2$^{142–252}$ with the subsequent modification of Thr154 (Fig. 2). Within experimental error, the heteronuclear ^{15}N-NOE values of the unmodified and modified forms of PntP2$^{142–252}$ are similar, indicating that phosphorylation does not dampen any fast timescale motions of amides in helix H0 (Fig. 3). Importantly, CLEANEX measurements also show that several residues in helix H0/H1 still undergo rapid HX in 2P-PntP2$^{142–252}$ and 3P-PntP2$^{142–252}$, albeit at a slightly reduced rate relative to the unmodified protein (Fig. 4). The average ~2.5-fold reduction in HX rate constants for corresponding residues in helix H0/H1 of 3P-PntP2$^{142–252}$ relative to the unmodified protein suggests that, in particular, pThr154 might marginally stabilize these helices by acting as an N-terminal cap.[36] However, chemical shift analyses by the MICS algorithm do not detect such a predominant role for either pThr151 or pThr154 (Fig. 2). Furthermore, the modest changes (particularly when viewed on a free energy scale) could be owing to electrostatic or inductive effects of a phosphothreonine on the intrinsic exchange rates of its neighboring residues,[31] or simply to subtle differences in experimental conditions as other amides in loop regions and at the C-terminus of the 3P-PntP2$^{142–252}$ also showed a comparable reduction in measured HX rate constants. Regardless, these experiments indicate that the structure and dynamics of PntP2$^{142–252}$ are perturbed minimally by phosphorylation.

MAP kinase docking by Pointed-P2

The interaction of PntP2$^{142–252}$ with ERK2 was also examined using ^{15}N-HSQC-monitored titrations. Upon addition of the unlabeled kinase, an overall decrease in the $^{1}N^{H}$–^{15}N signal intensities of amides throughout PntP2$^{142–252}$ was observed [Fig. 5(A,B)]. This is attributed to faster $^{1}N^{H}$ and ^{15}N transverse relaxation owing to the formation of a high-molecular-mass complex with the kinase. Based on the kinetic studies and equilibrium-binding measurements, the K_m or K_d values ERK2 kinases and PNT domains are in the range of 10–100 μM,[10,11,26] and thus partial saturation of PntP2$^{142–252}$ is expected under these experimental conditions. More importantly, residues in the phosphoacceptor region, as well as helices H0 and H5, showed substantially greater intensity changes yet no chemical shift perturbations. This suggests that these residues undergo pronounced exchange broadening[30] owing either to direct contacts with the kinase, as would be expected for the phosphoacceptors, or to indirect conformational perturbations. Indeed, when mapped on a homology model of PntP2$^{142–252}$, the residues in helices H0 and H5 are both in close proximity and adjacent to side chains in the PNT domain shown previously by mutagenesis to be involved in docking interactions with the ERK2 Rolled [Fig. 5(C)].[26] Similar results have also been observed for the interaction of the ETS1 PNT domain with ERK2.[10,39]

Discussion

Using NMR spectroscopy, we have examined the secondary structural and dynamic properties of a fragment of Pointed-P2, encompassing its phosphoacceptor region and adjacent PNT domain. Based on main chain chemical shifts, ^{15}N relaxation, and rapid amide HX measurements, the PNT domain of Pointed-P2 closely resembles that of ETS1 with a dynamic helix H0/H1 appended to a SAM core (helices H2–H5). Phosphorylation of three threonines in disordered N-terminal region of PntP2$^{142–252}$ does not significantly perturb the structure of its PNT domain and only slightly increases the protection of residues in helix H0/H1 against HX. Comparable subtle effects were observed for Ets1$^{29–138}$ when phosphorylated at Thr38 and Ser41.[4] However, as evidenced by changes in residual dipolar couplings and interproton NOE interactions, the dynamic helix H0 adopts a broad distribution of conformations in 2P-Ets1$^{29–138}$ that are more displaced from the PNT/SAM core than in the structural ensemble of unmodified Ets1$^{29–138}$.[4] This increased displacement is likely owing to electrostatic repulsion between pThr38/pSer41 and several negatively charged residues in helices H2 and H5. Given the sequence similarity of the two ETS family members, we speculate that such a conformational shift may also occur

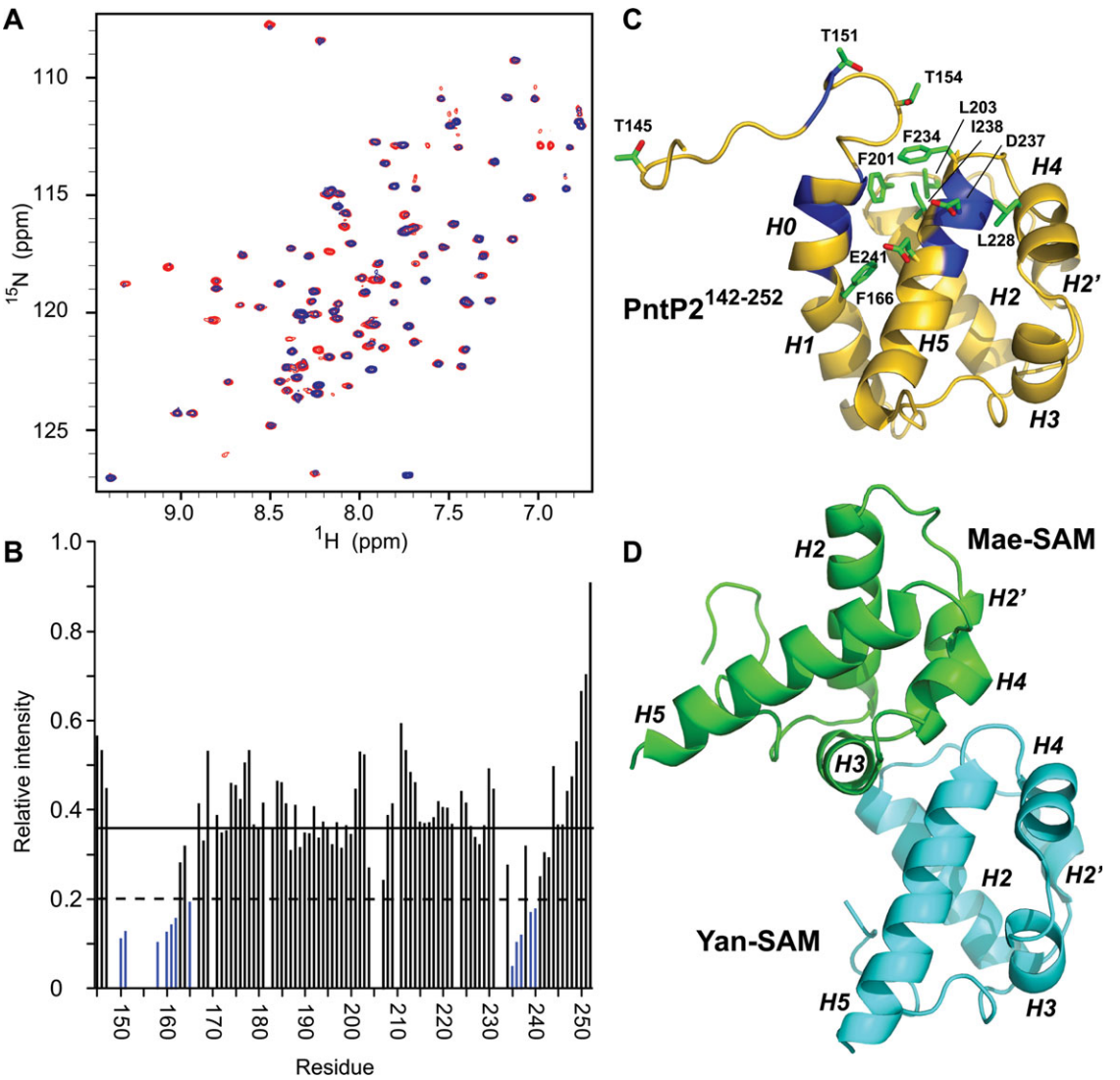

Figure 5. ERK2 interacts with the PNT domain and phosphoacceptor region of PntP2$^{142–252}$. (A) Superimposed ^{15}N-HSQC spectra of PntP2$^{142–252}$ at pH 7.5 in the absence (red) and presence (blue) of a 0.25 molar equivalent of active ERK2. (B) Addition of EKR2 leads to a significant reduction in the relative signal intensities of specific amides in the phosphoacceptor region, as well as in helices H0 and H5 of PntP2$^{142–252}$ (blue histogram bars). There is also an overall reduction in ^{5}N-HSQC signal intensities to an average value of ~0.4 (horizontal solid line) attributed to sample dilution and increased global relaxation rates owing to the formation of a high-molecular-mass complex. Missing data correspond to prolines, amides with overlapping signals, or residues not observed owing to rapid HX at the elevated sample pH of 7.5 that was required to prevent ERK2 aggregation. (C) The homology model of PntP2$^{142–252}$ generated with SwissModel[37] using Ets1$^{29–138}$ (2JV3.pdb) as a template. Amides showing the largest change in signal intensity upon ERK2 binding (below the horizontal dashed line in (B)) are highlighted in blue. Also shown in stick format (carbon, green; oxygen, red) are the side chains of residues identified by mutagenesis to be important for kinase docking,[26] as well as the three phosphoacceptors (Thr144, Thr151, and Thr154) and Phe166 at the H0/H1 bend. (D) X-ray crystallographic structure of the heterodimeric complex formed by the SAM/PNT domains of Mae (green) and Yan (cyan) (1SV0.pdb).[7] Binding of Mae to the corresponding region of PntP2$^{142–252}$ to prevent Rolled ERK2 docking would require displacement of the dynamic helix H0. The structural figures were rendered with PyMol.[38]

when Pointed-P2 is phosphorylated. Testing this hypothesis will, of course, require more detailed tertiary structural analyses of PntP2$^{142–252}$ in its unmodified and modified forms.

In addition to confirming that Thr151 is phosphorylated by ERK2, we also identified Thr145 and Thr154 as previously unrecognized phosphoacceptors adjacent to the PNT domain of Pointed-P2. Mutational studies have demonstrated that phosphorylation of Thr151 is critically required for the *in vivo* function of Pointed-P2,[18–20] whereas the biological roles, if any, of these additional nonconsensus sites have not been examined. It is certainly possible that these modifications are an artifact resulting from using a large scale *in vitro* kinase system to produce milligram quantities of modified PntP2$^{142–252}$ for NMR spectroscopic studies, and/or owing to differences between mammalian ERK2 and *Drosophila*

Rolled. However, the two MAP kinases are highly related, sharing 82% (89%) sequence identity (similarity), exhibit comparable docking interactions,[40] and function in homologous signaling cascades.[9,18,20] Furthermore, Ets1$^{29–138}$ is also phosphorylated *in vitro* by ERK2 at the corresponding Thr38 and Ser41, and *in vivo* tests have confirmed that both these residues contribute to Ras-enhanced transactivation by ETS1.[4,17] Thus, the potential roles of Thr145 and Thr154 in the control of gene expression by Pointed-P2 remain to be evaluated.

The results of this study have several implications for understanding the role of Pointed-P2 in the *Drosophila* signal transduction. Based on a mutational analysis, the Bowie group[26] identified several residues, centered around Phe234 at the start of helix H5, that contribute to the docking of Pointed-P2 and ERK2 Rolled [Fig. 5(C)]. Consistent with this analysis, amides within helix H5 showed pronounced spectral perturbations upon titration of PntP2$^{142–252}$ with ERK2. Furthermore, by comparison with the X-ray crystallographic structure of the Mae-SAM/Yan-SAM heterodimer [Fig. 5(D)],[7] these residues are also within the expected interface for Mae, thus leading to the proposal that Mae attenuates the activity of Pointed-P2 by sterically blocking kinase docking.[26] A homology model of PntP2$^{142–252}$, generated from the NMR spectroscopically derived structural ensemble of Ets1$^{29–138}$, predicts that helix H0 and the adjacent phosphoacceptors would partially occlude this interface [Fig. 5(C)]. If so, then the dynamic helix must be displaced to allow the binding of either ERK2 Rolled or Mae. This could lead to the ^{15}N-HSQC signal losses for residues in helix H0 observed when ERK2 was added to PntP2$^{142–252}$. Unfortunately, we found the isolated Mae PNT domain to be very insoluble *in vitro* and thus were unable to examine its predicted effect on PntP2$^{142–252}$ using NMR spectroscopy.

We speculate that the conformational flexibility and marginal stability of helix H0, detected by NMR relaxation and HX studies, might facilitate the phosphorylation of Pointed-P2 in two related ways. First, when folded, helix H0 positions the phosphoacceptors near the docking surface of the PNT domain, perhaps enhancing the initial association with the MAP kinase. Subsequently, the facile unfolding of this helix could then allow simultaneous interactions of the PNT domain with a docking site on the kinase and the phosphoacceptors with its active site to enable proximity-enhanced catalysis.[11] A similar proposal has been made for the interaction of ETS1 and ERK2.[4,16].

It is well established that phosphorylation of Pointed-P2 at Thr151 is necessary for the activation of its target genes.[18–21] However, the molecular mechanisms underlying this process have not been defined. By analogy to ETS1,[4,17] it is plausible that phosphorylation of Pointed-P2 leads to enhanced recruitment of Nejire, the *Drosophila* ortholog of the mammalian coactivator CBP. Although studies have shown that Nejire functions during successive stages of *Drosophila* eye development,[41] such a direct interaction with Pointed-P2 has not been reported. In an effort to test this hypothesis, we expressed the predicted TAZ1 domain of Nejire using a range of methods established for the TAZ1 domains of CBP and p300.[42] Unfortunately, we were unsuccessful in obtaining a soluble, folded protein fragment as required for NMR-monitored binding studies with PntP2$^{142–252}$. Therefore, future investigations will be required to uncover the link between Pointed-P2 phosphorylation and transcriptional activation. Our demonstration that the PNT domains and adjacent phosphoacceptors of ETS1 and Pointed-P2 share very similar secondary structural and dynamic properties should help guide this research.

Materials and Methods

Protein expression

The gene-encoding residues 142–252 of *D. melanoganster* Pointed-P2 (Genbank NM_079737.2) was cloned by PCR methods into the pET28a vector for expression in *Escherichia coli* BL21 (λDE3) cells as a His_6-tagged construct. The single cysteine (Cys250) was mutated to serine to avoid potential oxidation. Following established protocols,[4] the samples of $^{15}N/^{13}C$-labeled protein were produced in M9 minimal media, containing 1 g/L $^{15}NH_4Cl$ and 3 g/L $^{13}C_6$-glucose, with 1 m*M* isopropyl-β-D-thiogalactopyranoside (IPTG) induction overnight at 30°C. Harvested cells were resuspended and homogenized in lysis buffer (20 m*M* sodium phosphate, 500 m*M* NaCl, 5 m*M* imidazole, 2 m*M* dithiothreitol [DTT], pH 7.4) and the expressed protein isolated by Ni^{+2}-affinity chromatography, followed by thrombin digestion to remove the His_6-tag. After further purification using S75 size exclusion chromatography, the protein was dialyzed against NMR sample buffer (20 m*M* 3-(*N*-morpholino)-propanesulfonic acid, 10 m*M* NaCl, 2 m*M* DTT, pH 6.7) and concentrated by ultrafiltration. The resulting construct contains a non-native N-terminal Gly-Ser-His-Met from the cleavage site and is denoted as PntP2$^{142–252}$.

In vitro *phosphorylation*

PntP2$^{142–252}$ was phosphorylated by overnight incubation at 30°C in a 40:1 molar ratio with ERK2 kinase (125 m*M* Tris, 5 m*M* DTT, 50 m*M* $MgCl_2$, 100 m*M* NaCl, pH 7.5), as described previously for Ets1$^{29–138}$.[4] The active rat ERK2 was prepared from *E. coli* BL21 (λDE3) grown in TB media with 0.8% glycerol, 0.1 mg/mL carbenicillin, 0.08% glucose, and 0.04 m*M* IPTG for induction, according to the previously published methods.[10,17] The resulting 2P- and

3P-PntP2$^{142–252}$ were separated by anion exchange chromatography on a Mono Q column (20 m*M* Tris, pH 7.5, 10% glycerol, 2 m*M* DTT, gradient 0–1*M* NaCl), confirmed by MALDI-ToF mass spectrometry, and dialyzed into NMR sample buffer.

NMR spectroscopy

Spectra were obtained for proteins in NMR sample buffer with 10% D_2O at 25°C using 600 MHz Varian Inova or Bruker Avance III spectrometers. Data were processed with NMRpipe[43] and analyzed using Sparky.[44] Main chain resonance assignments were obtained using standard ^{15}N-HSQC, HNCO, HN(CA)CO, CBCA(CO)NH, HNCACB, and C(CO) TOCSY-NH experiments recorded with ^{1}H/^{13}C/^{15}N cryogenic probes.[45] The ^{1}H–^{15}N spectrum of a ^{31}P-edited HNCA experiment[32] was recorded using a room temperature ^{1}H/^{13}C/^{15}N/^{31}P QXI probe. Amide ^{15}N relaxation parameters[29] were obtained using a 600-MHz NMR spectrometer and analyzed using TENSOR2.[46] CLEANEX amide HX measurements[47] were recorded and analyzed as described previously.[4]

References

1. Hollenhorst PC, McIntosh LP, Graves BJ (2010) Genomic and biochemical insights into the specificity of ETS transcription factors. Annu Rev Biochem 80: 437–471.
2. Qiao F, Bowie JU (2005) The many faces of SAM. Sci STKE 2005:re7.
3. Mackereth CD, Scharpf M, Gentile LN, MacIntosh SE, Slupsky CM, McIntosh LP (2004) Diversity in structure and function of the Ets family PNT domains. J Mol Biol 342:1249–1264.
4. Nelson ML, Kang HS, Lee GM, Blaszczak AG, Lau DK, McIntosh LP, Graves BJ (2010) Ras signaling requires dynamic properties of ETS1 for phosphorylation-enhanced binding to coactivator CBP. Proc Natl Acad Sci USA 107:10026–10031.
5. Meruelo AD, Bowie JU (2009) Identifying polymer-forming SAM domains. Proteins 74:1–5.
6. Kim CA, Phillips ML, Kim W, Gingery M, Tran HH, Robinson MA, Faham S, Bowie JU (2001) Polymerization of the SAM domain of TEL in leukemogenesis and transcriptional repression. EMBO J 20:4173–4182.
7. Qiao F, Song H, Kim CA, Sawaya MR, Hunter JB, Gingery M, Rebay I, Courey AJ, Bowie JU (2004) Derepression by depolymerization; structural insights into the regulation of Yan by Mae. Cell 118:163–173.
8. Klambt C (1993) The *Drosophila* gene Pointed encodes two Ets-like proteins which are involved in the development of the midline glial cells. Development 117: 163–176.
9. Wasylyk C, Bradford AP, Gutierrez-Hartmann A, Wasylyk B (1997) Conserved mechanisms of Ras regulation of evolutionary related transcription factors, Ets1 and Pointed P2. Oncogene 14:899–913.
10. Seidel JJ, Graves BJ (2002) An ERK2 docking site in the Pointed domain distinguishes a subset of Ets transcription factors. Genes Dev 16:127–137.
11. Rainey MA, Callaway K, Barnes R, Wilson B, Dalby KN (2005) Proximity-induced catalysis by the protein kinase ERK2. J Am Chem Soc 127:10494–10495.
12. Abramczyk O, Rainey MA, Barnes R, Martin L, Dalby KN (2007) Expanding the repertoire of an ERK2 recruitment site: cysteine footprinting identifies the D-recruitment site as a mediator of Ets-1 binding. Biochemistry 46:9174–9186.
13. Callaway KA, Rainey MA, Riggs AF, Abramczyk O, Dalby KN (2006) Properties and regulation of a transiently assembled ERK2•Ets-1 signaling complex. Biochemistry 45:13719–13733.
14. Callaway K, Waas WF, Rainey MA, Ren PY, Dalby KN (2010) Phosphorylation of the transcription factor Ets-1 by ERK2: rapid dissociation of ADP and phospho-Ets-1. Biochemistry 49:3619–3630.
15. Piserchio A, Warthaka M, Devkota AK, Kaoud TS, Lee S, Abramczyk O, Ren P, Dalby KN, Ghose R (2011) Solution NMR insights into docking interactions involving inactive Erk2. Biochemistry 50:3660–3672.
16. Lee S, Warthaka M, Yan C, Kaoud TS, Piserchio A, Ghose R, Ren P, Dalby KN (2011) A model of a MAPK* substrate complex in an active conformation: a computational and experimental approach. PLoS One 6:e18594.
17. Foulds CE, Nelson ML, Blaszczak AG, Graves BJ (2004) Ras/mitogen-activated protein kinase signaling activates Ets-1 and Ets-2 by CBP/p300 recruitment. Mol Cell Biol 24:10954–10964.
18. Brunner D, Ducker K, Oellers N, Hafen E, Scholz H, Klambt C (1994) The Ets domain protein pointed-P2 is a target of MAP kinase in the sevenless signal transduction pathway. Nature 370:386–389.
19. O'Neill EM, Rebay I, Tjian R, Rubin GM (1994) The activities of two Ets-related transcription factors required for *Drosophila* eye development are modulated by the Ras/MAPK pathway. Cell 78:137–147.
20. Tootle TL, Rebay I (2005) Post-translational modifications influence transcription factor activity: a view from the Ets superfamily. Bioessays 27:285–298.
21. Vivekanand P, Rebay I (2006) Intersection of signal transduction pathways and development. Annu Rev Genet 40:139–157.
22. Vivekanand P, Tootle TL, Rebay I (2004) Mae, a dual regulator of the EGFR signaling pathway, is a target of the Ets transcription factors PNT and YAN. Mech Dev 121:1469–1479.
23. Tootle TL, Lee PS, Rebay I (2003) Crm1-mediated nuclear export and regulated activity of the receptor tyrosine kinase antagonist YAN require specific interactions with Mae. Development 130:845–857.
24. Song H, Nie M, Qiao F, Bowie JU, Courey AJ (2005) Antagonistic regulation of YAN nuclear export by Mae and Crm1 may increase the stringency of the Ras response. Genes Dev 19:1767–1772.
25. Baker DA, Mille-Baker B, Wainwright SM, Ish-Horowicz D, Dibb NJ (2001) Mae mediates MAP kinase phosphorylation of Ets transcription factors in *Drosophila*. Nature 411:330–334.
26. Qiao F, Harada B, Song H, Whitelegge J, Courey AJ, Bowie JU (2006) Mae inhibits Pointed-p2 transcriptional activity by blocking its MAPK docking site. EMBO J 25:70–79.
27. Vivekanand P, Rebay I The SAM domain of human TEL2 can abrogate transcriptional output from TEL1 (ETV-6) and ETS1/ETS2. PLoS One 7:e37151.
28. Shen Y, Bax A (2012) Identification of helix capping and β-turn motifs from NMR chemical shifts. J Biomol NMR 52:211–232.
29. Farrow NA, Muhandiram R, Singer AU, Pascal SM, Kay CM, Gish G, Shoelson SE, Pawson T, Forman-Kay JD, Kay LE (1994) Backbone dynamics of a free and phosphopeptide-complexed src homology 2 domain studied by ^{15}N NMR relaxation. Biochemistry 33:5984–6003.

30. Kleckner IR, Foster MP (2011) An introduction to NMR-based approaches for measuring protein dynamics. Biochim Biophys Acta-Proteins Proteomics 1814: 942–968.
31. Bai Y, Milne JS, Mayne L, Englander SW (1993) Primary structure effects on peptide group hydrogen exchange. Proteins 17:75–86.
32. McIntosh LP, Kang HS, Okon M, Nelson ML, Graves BJ, Brutscher B (2009) Detection and assignment of phosphoserine and phosphothreonine residues by ^{13}C-^{31}P spin-echo difference NMR spectroscopy. J Biomol NMR 43:31–37.
33. Bienkiewicz EA, Lumb KJ (1999) Random-coil chemical shifts of phosphorylated amino acids. J Biomol NMR 15:203–206.
34. Gonzalez FA, Raden DL, Davis RJ (1991) Identification of substrate recognition determinants for human ERK1 and ERK2 protein-kinases. J Biol Chem 266:22159–22163.
35. Songyang Z, Lu KP, Kwon YT, Tsai LH, Filhol O, Cochet C, Brickey DA, Soderling TR, Bartleson C, Graves DJ, DeMaggio AJ, Hoekstra MF, Blenis J, Hunter T, Cantley LC (1996) A structural basis for substrate specificities of protein ser/thr kinases: primary sequence preference of casein kinases I and II, NIMA, phosphorylase kinase, calmodulin-dependent kinase II, CDK5, and ERK1. Mol Cell Biol 16:6486–6493.
36. Andrew CD, Warwicker J, Jones GR, Doig AJ (2002) Effect of phosphorylation on alpha-helix stability as a function of position. Biochemistry 41:1897–1905.
37. Arnold K, Bordoli L, Kopp J, Schwede T (2006) The Swiss-model workspace: a web-based environment for protein structure homology modelling. Bioinformatics 22:195–201.
38. DeLano WL (2004) Use of Pymol as a communications tool for molecular science. Abstracts of Papers of the American Chemical Society 228:U313–U314.
39. Mackereth CD (2003) Structural and functional characterization of the PNT and SAM domains: diverse roles in protein-protein interactions. PhD Thesis, University of British Columbia.
40. Tanoue T, Adachi M, Moriguchi T, Nishida E (2000) A conserved docking motif in MAP kinases common to substrates, activators and regulators. Nat Cell Biol 2: 110–116.
41. Kumar JP, Jamal T, Doetsch A, Turner FR, Duffy JB (2004) CREB binding protein functions during successive stages of eye development in *Drosophila*. Genetics 168:877–893.
42. De Guzman RN, Wojciak JM, Martinez-Yamout MA, Dyson HJ, Wright PE (2005) Cbp/p300 TAZ1 domain forms a structured scaffold for ligand binding. Biochemistry 44:490–497.
43. Delaglio F, Grzesiek S, Vuister GW, Zhu G, Pfeifer J, Bax A (1995) NNMpipe—a multidimensional spectral processing system based on Unix pipes. J Biomol NMR 6:277–293.
44. Goddard TD, Kneeler DG (1999) Sparky, 3rd ed. San Francisco: University of California.
45. Sattler M, Schleucher J, Griesinger C (1999) Heteronuclear multidimensional NMR experiments for the structure determination of proteins in solution employing pulsed field gradients. Prog Nucl Mag Reson Spect 34: 93–158.
46. Dosset P, Hus JC, Blackledge M, Marion D (2000) Efficient analysis of macromolecular rotational diffusion from heteronuclear relaxation data. J Biomol NMR 16: 23–28.
47. Hwang TL, van Zijl PC, Mori S (1998) Accurate quantitation of water-amide proton exchange rates using the phase-modulated clean chemical exchange (CLEANEX-PM) approach with a fast-HSQC (fHSQC) detection scheme. J Biomol NMR 11:221–226.